In situ chemical sensing in AlGa*N*/GaN metal organic chemical vapor deposition process for precision film thickness metrology and real-time advanced process control

Soon Cho,[a] Daniel S. Janiak, and Gary W. Rubloff[b]
Department of Materials Science and Engineering and Institute for Systems Research, University of Maryland, College Park, Maryland 20742

Michael E. Aumer, Darren B. Thomson, and Deborah P. Partlow
Advanced Materials and Semiconductor Device Technology Center, Northrop Grumman Electronic Systems, Linthicum, Maryland 21090

(Received 7 January 2005; accepted 18 July 2005; published 14 September 2005)

In situ mass spectrometry is implemented in AlGaN/GaN/AlN metalorganic chemical vapor deposition processes on SiC substrates as a real-time process- and wafer-state metrology tool. Dynamic chemical sensing through the process cycle, carried out downstream from the wafer, revealed generation of methane and ethane reaction by-products as well as other residual gas species. The methane and ethane by-products are believed to reflect the two parallel chemical reaction pathways leading to GaN-based materials growth, namely the gas phase adduct formation route and the direct surface decomposition of the metalorganic precursor, respectively. Having detected both types of by-products as evidence for the presence of both paths, we monitored and integrated the methane and ethane signals to derive a real-time film thickness metric. Integrating the sum of the two by-product signals in this manner through the AlGaN growth period (~1 min or less) enabled us to predict the AlGaN cap layer thickness (~20 nm) to within ~1% or ~0.2 nm precision. This was verified by postprocess x-ray reflectance measurement, which produced a thickness map over the 2 in. wafer and yielded an average thickness for the AlGaN cap layer for comparison to the real-time mass spectrometry. These results demonstrate an opportunity for advanced process control based on real-time *in situ* chemical sensing, with the promise of major benefit in reproducibility and cost reduction in AlGaN/GaN-based semiconductor manufacturing. © *2005 American Vacuum Society.* [DOI: 10.1116/1.2037707]

I. INTRODUCTION

Gallium nitride (GaN) and its alloys promise to be key materials for future semiconductor devices aimed at high frequency, high power electronic applications (e.g., radar applications).[1–3] However, manufacturing for such high performance products requires systematic methodology to achieve reproducible metrics such as material quality and film thickness across the heterostructure. In particular, controlling the aluminum gallium nitride (AlGaN) cap layer thickness is known to be a critical parameter directly affecting the device performance. To this end, better understanding of the complex process chemistries involved and an emphasis on *advanced process control* (APC) are viewed as being highly desirable at the current stage of technology's evolution.

APC has already been widely accepted in the Si ultralarge scale integration (ULSI) industry, both in terms of *fault detection and classification* (FDC), and *course correction*.[4,5] Our research group has been an active contributor in various aspects of APC, especially in the use of real-time *in situ* chemical sensors for both FDC and course correction.[6–16] Understanding the relevant challenges currently facing the development of GaN-based processes for manufacturing in electronic applications, we have applied similar APC approaches based on our past experience in Si-based processes, in hopes of achieving process reproducibility sufficient for manufacturing.[17,18] We have employed *in situ* mass spectrometry (mass spec) in AlGaN/GaN/AlN metalorganic chemical vapor deposition (MOCVD) processes, initially devoted to numerous FDC applications,[19] and subsequently to development of quantitative metrologies for predicting/controlling material qualities[20] and film thickness.

A number of important material design parameters must be optimized and controlled based on the particular design of the GaN-based high electron mobility transistor (HEMT) heterostructure for our advanced microwave electronics application. Naturally, the particular heterostructure design dictates the processing sequence, which for us, consisted of growing the following three layers on semi-insulating (resistivity >1E5 Ω-cm) 4H–SiC(0001) substrates (2 in. diam): ~100-nm-thick AlN nucleation layer, ~1-μm-thick GaN epilayer, and 20–25-nm-thick AlGaN cap layer. The individual layer thicknesses, crystal quality, and impurity content must be carefully optimized and controlled across the heterostructure, because they affect the two-dimensional electron gas concentration, background carrier concentration, their mobilities, etc.[21] (Also, see our companion publication[20] for de-

[a]Current address: Intel Corporation, electronic mail: soon.cho@intel.com
[b]Author to whom correspondence should be addressed; electronic mail: rubloff@isr.umd.edu

TABLE I. Process and tool conditions used for the AlGaN part of the AlGaN/GaN/AlN HEMT heterostructure growth runs.

Run No.	AlGaN time (s)	Pressure (Torr)	Carrier gas (slm)	NH_3 (slm)	TMG (sccm)	TMA (sccm)	Pyrometer T. (°C)	Showerhead	Liner
G288	259	50	25	4	5	12	1107	F	10
G289	259	50	25	4	6	12	1108	F	10
G290	260	50	25	4	7	12	1115	F	10
G379	180	50	15	3	15	24	1111	G	3
G380	138	50	15	3	15	24	1102	G	3
G383	77	50	15	3	20	44	1106	G	12
G386	80	50	15	3	20	47	1113	G	18
G387	59	50	15	3	20	47	1107	G	18
G406	65	50	15	3	16	46	1147	F	9
G409	64	50	15	3	15	38.3	1140	F	14
G413	58	50	15	3	19	55	1138	F	17
G416	54	50	15	3	20	48	1126	F	12

tails of the heterostructure design issues.) In particular, the AlGaN cap layer thickness (d), which is the subject of this article, must be precisely optimized and controlled because it directly affects the final device performance in terms of transconductance (g_m) and the frequency of unit current gain (f_T) as follows:[22,23]

$$f_T \propto g_m \propto \frac{1}{d}. \tag{1}$$

We report here the development of a working real-time metric (based on the methane and ethane by-product signals from mass spec) for accurately predicting the AlGaN cap layer thickness during growth (precision ~1%) with the corresponding metrology models that can be used to drive real-time end-point control in these processes.

II. EXPERIMENTS

A. HEMT heterostructure growth by MOCVD

Details of the experimental process conditions and equipment descriptions are published elsewhere[20] and only a summary is presented here. All experiments were carried out within a water-cooled quartz-wall reactor (custom designed), which includes a quartz liner inside a double quartz furnace wall. The system was equipped with a commercial gas delivery system supplied by EMF. Reactants [NH_3, trimethylaluminum (TMA), and trimethylgallium (TMG)] with the carrier gas (H_2) were delivered through two quartz delivery tubes fused to a custom designed quartz showerhead. In particular, the metalorganic precursors (TMA and TMG) and NH_3 were kept separated in their respective delivery tubes until they reached the showerhead, at which point they intermixed uniformly within the showerhead before being delivered to the wafer region below. Single wafer substrate (2-in.-diam semi-insulating SiC from Cree) was placed on the SiC-coated graphite susceptor, which was inductively heated at 10 kHz to provide heating for the film growth to occur on the wafer. The residual process gases were continuously pumped away through the exhaust lines located at both ends of the reactor, connected to a common rotary vane pump.

All three layers of the HEMT heterostructure, as described in Sec. I, were grown sequentially within the same process, and an *in situ* mass spec was used to monitor the progress in real time. Overall, the limited number of runs (12) reflects the inherently limited throughput using the costly semi-insulating SiC wafers. The exact process and tool conditions used for the runs are summarized in Table I. The continuous variation in process parameters reflects the efforts to optimize the process conditions for improved material quality, while the use of different showerhead designs (different hole pattern, size, and distribution) reflects the efforts to improve growth uniformity through continuous showerhead model refinement as discussed in our other publications.[24] Typically, the TMG and TMA flow rates and the growth temperature were varied while the total pressure, carrier gas, and NH_3 gas flow rates were maintained constant run to run. The process temperature set point (as measured via a sapphire light pipe directed at the bottom of the susceptor) was intentionally varied, and the actual temperature was confirmed by an independent optical pyrometer aimed at one side of the susceptor, which is reported in Table I.

B. Real-time *in situ* process sensing by mass spectrometry

The schematic layout of the mass spec sampling system, integrated to the MOCVD tool, is published elsewhere.[20] The process and residual gases were sampled directly from the reactor downstream via a 1/16-in.-o.d. × 0.010-in.-i.d. × 20-cm-long stainless steel capillary, which resulted in a pressure drop from the process pressure of 50 Torr down to ~1 Torr behind the capillary. Most of this gas was then pumped away by a bypass differential pumping to the foreline of the diaphragm pump (backing pump for the mass spec's turbo-molecular pump), leaving only a small fraction

of the gas to enter a 20-μm-i.d. orifice into the closed ion source region of the mass spec (Inficon model CPM™, 200 amu quadrupole mass spec).

By using an appropriately sized capillary-orifice combination for the gas conductance network, the sampled gas pressure was reduced from the viscous flow regime (50 Torr) to the molecular flow regime (~1 Torr). The bypass differential pumping technique enabled us to actively withdraw gases from the process through the sampling system. Both of these sampling techniques, as well as the location of the sampling capillary (i.e., within the main gas flow downstream to the growth reaction), were critical in achieving adequate response time in process sensing, which is needed for real-time process control application discussed here.

The W filament current in the closed ion source was kept at 200 μA, while the electron energy was maintained at 40 eV. This provided adequate sensitivity and minimum parasitic reactions within the closed ion source region. Electron multiplier detection was used at acceleration voltages of 1160 V (for runs G288–G290), 835 V (for runs G379–G409 after the electron multiplier unit was replaced), and 840 V (for runs G413–G416) to enhance and maintain the signal-to-noise ratio run to run.

C. Postprocess material characterizations

The samples grown on SiC substrates as described in the preceding sections were examined using a number of postprocess characterization techniques, including x-ray reflectance (XRR), x-ray diffraction (XRD), and photoluminescence. In particular, the XRR was performed using a Bede D1™ system equipped with a microsource for higher spatial resolution. Separation of interference fringes from the reflectance signals was used by the automated software to deduce the AlGaN cap layer thickness at each point as follows:[25]

$$\Delta\theta = \frac{\lambda \gamma_g}{t \sin(2\theta_B)}, \tag{2}$$

where $\Delta\theta$ is the interference fringe separation, λ is the x-ray wavelength, γ_g is the cosine of the angle between the diffracted beam and the inward-going normal to the sample surface, t is the layer thickness, and θ_B is the Bragg angle for diffraction. Measurements were made at 42 points on a polar coordinate grid over the 2 in. wafer to generate a wafer-wide contour fit map for the AlGaN thickness and a corresponding histogram (area weighted) as shown in Fig. 1. The average value from the histogram was then used as a measure of the average AlGaN thickness reported in this article.

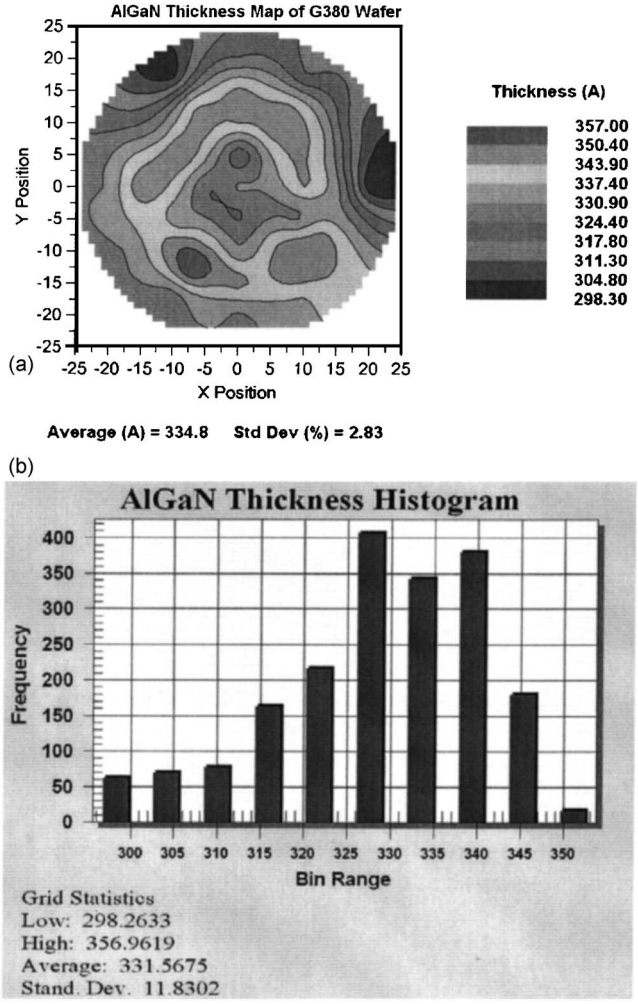

FIG. 1. XRR thickness map and histogram. Measurements were made at 42 points on a polar coordinate grid over the 2 in. wafer to generate (a) a wafer-wide contour fit map for the AlGaN cap layer thickness and (b) the corresponding histogram. The average value from the histogram was then used as a measure of the average AlGaN thickness reported in this article. Note that this is an area-weighted average value. This example is taken from run G380, for which the equipment configurations and process conditions are described in Table I.

III. RESULTS

A. Chemical sensing

In situ mass spec sensing of the 50 Torr MOCVD growth process as described above provided dynamic, real-time gas phase chemical signals as a function of the process cycle. Figure 2 shows the characteristic ion current signals, through the entire process cycle, from H_2 (carrier gas), NH_3 (column V precursor), N_2 (fragmentation product from NH_3), H_2O (background impurity), CH_4 (reaction byproduct), C_2H_6 (reaction by-product), C (background impurity), and O_2 (background impurity). Virtually no column III precursors (TMA and TMG) were detectable in their original chemical form at the downstream location. This is primarily attributed to the close to complete decomposition and utilization at the extremely high growth temperature near the wafer and showerhead regions. Note also that for the reaction by-products CH_4 (methane) and C_2H_6 (ethane) mass peaks at 13 and 26 amu's (atomic mass units) were used instead of 16 and 30 amu's as one might expect. These values were chosen from components in the fragmentation patterns of the parent species to minimize ambiguity where mass fragments from multiple sources overlap.

Moreover, it is believed that the two by-products, methane and ethane, originate from the two *parallel* chemical reaction pathways to grow GaN-based material on the wafer as dis-

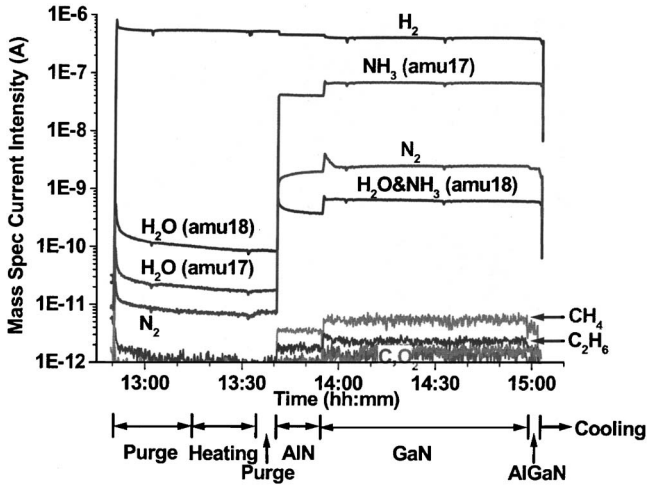

FIG. 2. *In situ* gas phase chemical signals from mass spec, indicative of the dynamic gas composition downstream of the reactor as a function of process steps. The mass spec current signals were acquired in real time through the entire HEMT growth process.

cussed in our companion publication.[20] One occurs through complex adduct species formation in the gas phase to form a trimer specie before finally decomposing to form GaN (or AlGaN, depending on precursors) on the hot wafer surface. This adduct pathway releases several molecules of methane as the reaction by-product. On the other hand, the metalorganic precursor(s) can decompose directly in the gas phase to grow GaN (or AlGaN), releasing primarily ethane as its reaction by-product. In our companion publication,[20] we showed that the methane/ethane ratio, obtained in real time during growth, can successfully predict the crystal quality of the GaN epilayer with quantitative precision (1%–5%), which is verified by postprocess XRD measurement of crystal quality. In that situation, the by-products ratio reflected the relative amount of material produced by either path, which yields different material quality. We also note that since the two by-products come from two different *parallel* pathways to grow the GaN-based material on the wafer, it is expected that summing the two by-product signals over the duration of the film growth provides a measure related to the total film thickness grown. Hence, we have applied this methodology to real-time AlGaN cap layer thickness metrology here.

B. Real-time metric development

Although we initially observed a reasonable quantitative correlation to the AlGaN thickness using the raw mass spec current signals measured at 13 and 26 amu's, additional efforts were made to more accurately model the relationship between the real-time mass spec signals and the postprocess XRR measurement of the actual film thickness, thus improving the precision of the real-time metrology model. In particular, by incorporating different normalization factors (α and β) described below for the raw methane and ethane signals enabled better approximation for the species' true relative partial pressures, thus ensuring that the model is insensitive to the relative contributions of methane versus ethane paths. Additionally, normalization with respect to the 50 Torr H_2 signal measured prior to each run corrected for any sensor drifts.

Equation (3) describes the relationship between the partial pressure of substance "*a*" (PP_a) and the raw mass spec ion current for the substance at mass "*b*" (I_{ab}). Basically, there are two factors relating the raw ion current observed to the true partial pressure of the substance: (1) the *material factor* (M_{ab}) which depends on the nature of the substance being detected and (2) the *analyzer factor* (A_b) which depends on the characteristics of the partial pressure analyzer[26]

$$PP_a = (M_{ab} \times A_b) \times I_{ab}. \tag{3}$$

The material factor (M_{ab}), further depends on the fragmentation pattern for the particular substance and the reference gas (usually nitrogen), and the ease with which the substance can be ionized relative to the same reference gas as shown in the following equation:[26]

$$M_{ab} = (FF_{ab} \times XF_a)^{-1}. \tag{4}$$

The term FF_{ab} is the *fragmentation factor* for substance *a* at mass *b*. It is equal to the fraction of the total current of all ions from substance *a* which has a mass *b*. The term XF_a is the *ionization probability* of substance *a* relative to nitrogen (i.e., $XF_N = 1$), otherwise known as the relative *cross section* of the substance. It is the ratio of total ion current (for all masses) from substance *a* to the total ion current from nitrogen, both measured at the same true partial pressure. The *FF's* for methane at amu 13 and ethane at amu 26 were estimated to be 0.04 and 0.12, respectively, based on the fragmentation patterns obtained from the National Institute of Standards and Technology (NIST) database.[27] Likewise, the *XF* values were obtained by taking the absolute cross sections of methane (0.2975 nm) and ethane (0.5518 nm), then dividing them by that of nitrogen (0.1812 nm), which gave 1.642 for methane and 3.045 for ethane. From the *FF's* and *XF's*, *M's* could be calculated using Eq. (4). However, the *A's* were far more difficult to obtain. Hence, we only considered the *M's* for methane (at amu 13) and ethane (at amu 26) here, whose values were calculated to be 15.225 and 2.737, respectively. Multiplying the methane and ethane raw mass spec signals with the respective material factors provides the following expression:

$$\alpha \int S(\mathrm{CH_4})dt + \beta \int S(\mathrm{C_2H_6})dt, \tag{5}$$

where $\alpha(15.225)$ and $\beta(2.737)$ are the material factors for methane (at amu 13) and ethane (at amu 26), respectively, and $\int S(\mathrm{CH_4})$ and $\int S(\mathrm{C_2H_6})$ represent the raw mass spec current signals for methane (at amu 13) and ethane (at amu 26) integrated in real time over the AlGaN growth step as shown in Fig. 3. Note that the changes in mass spec signal levels exhibit the characteristic response time of the system (e.g., delayed signal rise in the beginning of AlGaN and prolonged decay during cooling). The rationale for setting the upper and lower limits of integration using the equipment-state signals

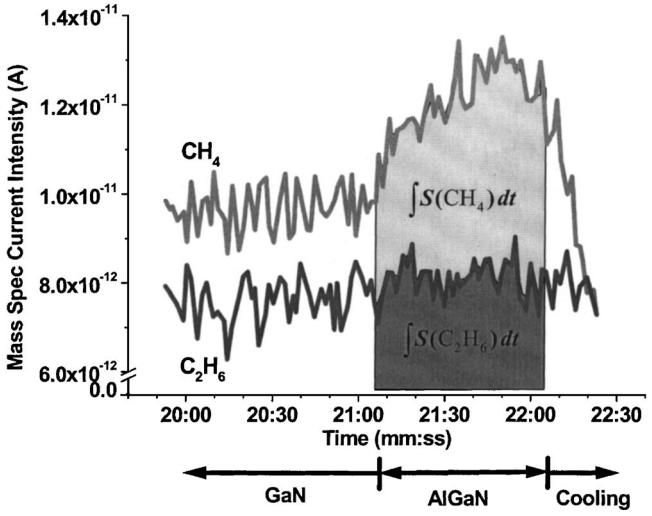

FIG. 3. *In situ* methane and ethane signals from mass spec during an AlGaN cap layer growth period. The current growth step (i.e., GaN or AlGaN) was determined from the relevant equipment-state changes (e.g., TMA line open/close signal). Areas under each curve were integrated over the duration of the AlGaN growth period to generate the real-time film thickness metric. Note that in this case the ethane signal did not produce a noticeable change in magnitude going from GaN to AlGaN layer growth, which seem to indicate that the ethane by-product, thus the surface reaction path, may be relatively insensitive to the TMA-based chemistry. However, further study is required for clearer understanding of the chemistry.

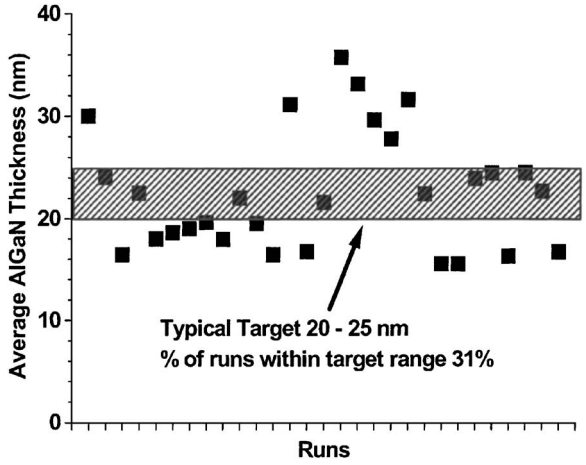

FIG. 4. Run-to-run variation in product AlGaN cap layer thickness as determined by XRR. Shown are the data from all HEMT heterostructure growth runs performed on semi-insulating SiC substrates during an arbitrary period in the year 2003. Considering that typical thickness process windows are in the range of 20–25 nm, these runs could imply a yield as low as ~31%.

(i.e., TMA line open/close signals) is that by being systematic and consistent in the manner by which the metrology signal is calculated each time, and assuming the system response time is more or less constant run to run, the overall metrology precision is not expected to be compromised.

The values obtained from Eq. (5) were then normalized with respect to the 50 Torr H_2 current signal measured at amu 2 prior to the growth step for each run. This was an attempt to correct for the minor sensor drifts, for example, the slight run-to-run variation in signal gain and sensor sensitivity. Finally, our real-time metric for predicting the AlGaN thickness becomes

$$\frac{1}{S(\mathrm{H_2})}\left[\alpha\int S(\mathrm{CH_4})dt+\beta\int S(\mathrm{C_2H_6})dt\right]. \tag{6}$$

Comparison of the normalized signal to the postprocess XRR measurement of AlGaN thickness generated a precision film thickness metrology model as discussed in the following sections. Furthermore, the mass spec based signal could now be used as our real-time film thickness metric to predict the AlGaN cap layer thickness during growth to a precision defined by the model.

C. AlGaN thickness variability and metrology under varying process/equipment conditions

In terms of thickness control for the various layers within the heterostructure, controlling the AlGaN cap layer thickness is the greatest challenge. It is the thinnest layer, with a typical target thickness range of 20–25 nm. Figure 4 shows the run-to-run variation in the average AlGaN thickness measured by XRR for the HEMT heterostructure growth runs on semi-insulating SiC substrates performed without control. Unfortunately, not more than 1/3 of the runs fell within the target range of 20–25 nm, reflecting the large intentional process and equipment variability. Even using the same exact tool configuration run to run, we observed that multiple process adjustments and wafers were necessary to reach a given target.

Figure 5 shows the real-time sensor-based AlGaN thickness metric [see Eq. (6)] compared to the actual film thickness measured by postprocess XRR. Linear regression model between the real-time sensor-based metric and postprocess XRR measurement indicates a precision of 3.9% or 1.0 nm average uncertainty. This is a reasonable precision considering that it represents a broad thickness variation (~2X), un-

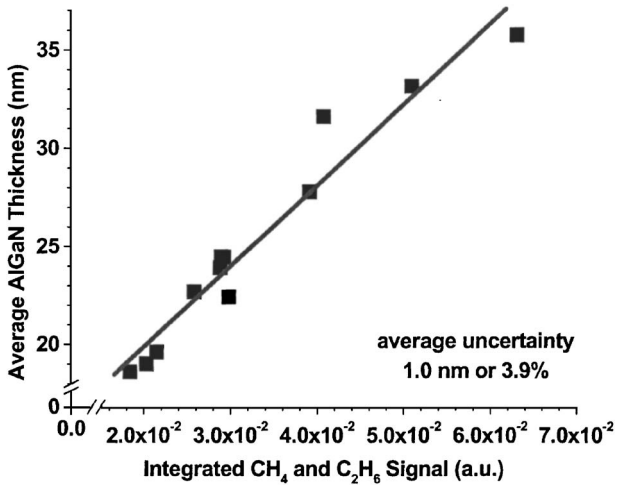

FIG. 5. AlGaN cap layer thickness metrology over a broad thickness range ($\Delta \sim 17$ nm). The real-time film thickness metric based on methane and ethane signals measured by mass spec exhibited a strong linear correlation (3.9% precision) to the actual film thickness grown, as measured by postprocess XRR.

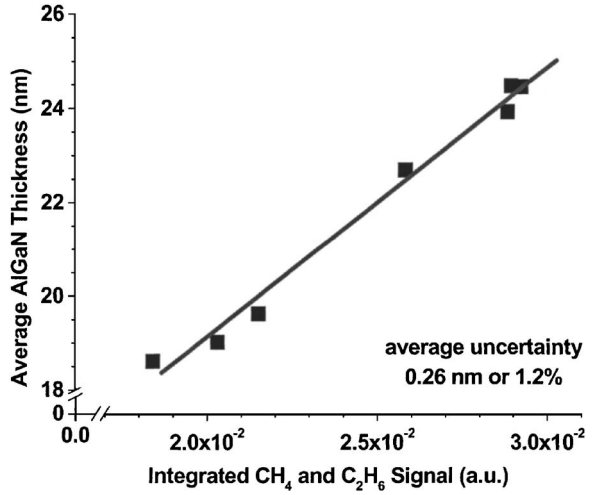

FIG. 6. AlGaN cap layer thickness metrology within the thickness range of ~6 nm. The real-time film thickness metric based on methane and ethane signals measured by mass spec exhibited a strong linear correlation (1.2% precision) to the actual film thickness grown, as measured by postprocess XRR.

likely to be encountered in high volume manufacturing typically with fixed tool configurations and process conditions.

Note that Fig. 4 is not intended to demonstrate irreproducibility/reproducibility of given *fixed* process/equipment conditions. Rather, it shows our efforts to achieve the desired AlGaN thickness target (which we always know to be in the range of 20–25 nm), concurrent with various *intentional* changes made in process/equipment conditions inherent to the technology development process (as discussed already in Sec. II A). No doubt, fixed mature process/equipment conditions (as in a high volume manufacturing situation) would ultimately be desirable, because we would then expect a *relatively* tighter variation in film thicknesses as well as other material quality metrics—even without an *in situ* metrology/control. However, the value of *in situ* metrology as developed here lies in the fact that even with uncertainties introduced by intentional process/equipment changes (for optimization of other critical film properties, for example), thickness is predictable—in *real time* and with reasonable *precision*.

D. Precision thickness metrology for manufacturing under fixed process/equipment conditions

While the experiments above included a variety of process conditions and equipment configurations, we would also like to assess the prognosis for real-time thickness metrology and control, where equipment configurations will be fixed and nominal process settings relatively invariant. To *estimate* the metrology precision, we therefore filtered the data in Fig. 5 to specify fixed equipment and process conditions. Filtering the metrology data to restrict it to a single showerhead design (F) and a more restricted thickness range (19–25 nm), we are left with seven data points as shown in Fig. 6. Linear regression model based on the local range data yields a precision of 1.2% or 0.26 nm. This local range metrology result demonstrates a striking level of precision for AlGaN cap layer thickness metrology: if translated into real-time end-point control, it suggests that a 20 nm cap layer could be controlled to 0.2 nm in the presence of 20%–30% process and equipment variability.

IV. DISCUSSION

The AlGaN cap layer thickness metrology developed here demonstrates sufficient precision for use in manufacturing process control (in addition to its existing application in our technology development efforts), for example, in the form of run-to-run or—more straightforwardly and effectively—real-time process control. The mass spec sensor is particularly attractive because it can be used to serve other important purposes such as FDC[19] and process learning,[20] which are reported elsewhere. The use of mass spec for manufacturing process control has already been well demonstrated in the past, for example, in a 10 Torr W CVD process.[16]

In this work, we have demonstrated that the same mass-spec-based thickness metrology and control can be extended into the nanoscale regime. For instance, the AlGaN cap layer (~20 nm) here is orders of magnitude thinner than the blanket W layer (>1 μm) in the W CVD process.[16] This is important because the Si ULSI industry is now dealing with various kinds of ultrathin (nanoscale) layers, such as barrier layers or gate dielectrics by CVD or atomic layer deposition[28]—a challenging requirement for the precision of *in situ* sensors. Not a traditional thickness monitoring sensor, mass spec metrology demonstrated here achieves nm—even atomic—precision.

Moreover, the level of methane and ethane signals here were on the order of ppm or less (relative to the largest signal, H_2 carrier gas) as seen in Figs. 2 and 3. In the previous work observing the HF by-product in W CVD process, the reaction product was on the order of ~10% of the largest signal, the H_2 reactant.[16] Despite the low signal levels in the present work on AlGaN MOCVD, significant precision was achieved, in part by implementing special measures such as the use of electron multiplier detection, different dwell times as a function of species detection levels, and run-to-run data normalization for any sensor sensitivity drift. As a result, both the thinner thickness and lower species detection levels have been successfully overcome without a significant loss in control capability here.

In fact, the ~1% metrology precision has been deemed sufficient to drive end-point process control. Although no data are currently available from a dedicated series of control experiments, a cruder form of end-point control has been routinely implemented in our AlGaN/GaN/AlN MOCVD processes. It indicates the control precision to be ~1%–2% to date, which in turn increased the yield of the particular unit process step from ~31% as seen in Fig. 4 to near > ~90% with control. Meanwhile, a more complete interfacing of the sensor, MOCVD tool, and the tool controller has been realized with a LabVIEW™-based process control program (custom programmed by the authors) sharing the data in real time with the other components through DDE™-

based communication. This enables a complete closed-loop automated process control based on precision metrology as developed here. More is to be discussed in future publications related to the control of these processes. This offers important benefits in terms of the reduced number of manual process recipe tuning runs (performed on *n*+ substrates prior to growth on semi-insulating substrates), significant cost savings from reduced number of wasted runs/wafers, and the limited throughput in current tool set.

V. CONCLUSIONS

In situ mass spec sensing was implemented in 50 Torr AlGaN/GaN/AlN HEMT heterostructure growth processes in order to enhance and control process reproducibility, and to achieve better understanding of the intrinsic chemistry involved. Dynamic chemical sensing through the process cycle, carried out downstream from the wafer, revealed generation of methane and ethane reaction by-products in real time, in addition to other residual gas species present in the process. The methane and ethane by-products are believed to reflect the two parallel reaction pathways leading to GaN-based materials growth, namely the gas phase adduct formation route and the direct surface decomposition of the metal-organic precursor, respectively. Assuming that both pathways contribute in the MOCVD process, we monitored and integrated the methane and ethane signals in real time to derive a real-time film thickness metric. Integrating the sum of the two by-product signals in this manner through the AlGaN growth period (~1 min or less) enabled us to predict the AlGaN cap layer thickness (~20 nm) to within ~1% or ~0.2 nm precision. This was verified by postprocess XRR measurements averaged over the 2 in. wafer.

The use of mass spec for manufacturing process control has already been well demonstrated in the past, for example, in a 10 Torr W CVD process by the authors. However, the AlGaN cap layer thickness metrology developed here represents a significant improvement in capability of such *in situ* sensor-based process- and wafer-state metrology, namely thickness precision at atomic scale (and 1% of total thickness) using by-product signals at the ppm levels. Furthermore, ~1% metrology precision has been deemed sufficient to drive real-time end-point process control, and it is currently implemented and used routinely in our AlGaN/GaN/AlN MOCVD processes. This offers important benefits in terms of the reduced number of manual process recipe tuning runs, significant cost savings from reduced number of wasted runs/wafers, and the limited throughput available in our development tool set.

In summary, these results demonstrate an opportunity for advanced process control based on real-time *in situ* chemical sensing, with the promise of major benefit in reproducibility and cost reduction in AlGaN/GaN-based semiconductor manufacturing.

ACKNOWLEDGMENTS

The authors are grateful for a close research partnership with, and financial support from, the Northrop Grumman Corporation. The authors also appreciate continuing interaction and technical support from Inficon, Inc., particularly R. Ellefson and L. Frees. Inficon is a supplier of mass spectrometric sensors for process control applications in semiconductor manufacturing processes.

[1]L. F. Eastman and U. K. Mishra, IEEE Spectrum **5**, 28 (2002).
[2]U. K. Mishra, P. Parikh, and Y. Wu, Proc. IEEE **90**, 1022 (2002).
[3]R. J. Trew, Proc. IEEE **90**, 1032 (2002).
[4]T. Sonderman, M. Miller, and C. Bode, Future Fab International **12**, 119 (2002).
[5]S. W. Butler, J. Vac. Sci. Technol. B **13**, 1917 (1995).
[6]L. L. Tedder, G. W. Rubloff, I. Shareef, M. Anderle, D.-H. Kim, and G. N. Parsons, J. Vac. Sci. Technol. B **13**, 1924 (1995).
[7]L. L. Tedder, G. W. Rubloff, B. F. Cohaghan, and G. N. Parsons, J. Vac. Sci. Technol. A **14**, 267 (1996).
[8]A. I. Chowdhury, W. W. Read, G. W. Rubloff, L. L. Tedder, and G. N. Parsons, J. Vac. Sci. Technol. B **15**, 127 (1997).
[9]G. Lu, L. L. Tedder, and G. W. Rubloff, J. Vac. Sci. Technol. B **17**, 1417 (1999).
[10]T. Gougousi, Y. Xu, J. N. Kidder, Jr., G. W. Rubloff, and C. R. Tilford, J. Vac. Sci. Technol. B **18**, 1352 (2000).
[11]L. Henn-Lecordier, J. N. Kidder, Jr., G. W. Rubloff, C. A. Gogol, and A. Wajid, J. Vac. Sci. Technol. A **19**, 621 (2001).
[12]R. Sreenivasan, T. Gougousi, Y. Xu, J. Kidder, Jr., E. Zafiriou, and G. W. Rubloff, J. Vac. Sci. Technol. B **19**, 1931 (2001).
[13]Y. Xu, T. Gougousi, L. Henn-Lecordier, Y. Liu, S. Cho, and G. W. Rubloff, J. Vac. Sci. Technol. B **20**, 2351 (2002).
[14]L. Henn-Lecordier, J. N. Kidder, Jr., G. W. Rubloff, C. A. Gogol, and A. Wajid, J. Vac. Sci. Technol. B **21**, 1055 (2003).
[15]S. Cho, L. Henn-Lecordier, A. Singhal, Y. Xu, Y. Liu, J. N. Kidder, Jr., and G. W. Rubloff, in *AEC/APC Symposium XV*, edited by International Sematech (International Sematech, Austin, TX, 2003), Cho_Soon-SP2595.
[16]S. Cho, L. Henn-Lecordier, Y. Liu, and G. W. Rubloff, J. Vac. Sci. Technol. B **22**, 880 (2004).
[17]S. Cho, G. W. Rubloff, M. E. Aumer, D. B. Thomson, and D. P. Partlow, presented at the AVS 50th International Symposium, Baltimore, MD, 2003 (unpublished).
[18]S. Cho, G. W. Rubloff, M. E. Aumer, D. B. Thomson, and D. P. Partlow, presented at the Materials Research Society Fall Meeting, Boston, MA, 2003 (unpublished).
[19]S. Cho, G. W. Rubloff, M. E. Aumer, D. B. Thomson, and D. P. Partlow, J. Vac. Sci. Technol. B **23**, 1849 (2005).
[20]S. Cho, G. W. Rubloff, M. E. Aumer, D. B. Thomson, D. P. Partlow, R. Parikh, and R. A. Adomaitis, J. Vac. Sci. Technol. B **23**, 1386 (2005).
[21]H. Morkoc, *Nitride Semiconductors and Devices* (Springer, Berlin, 1999).
[22]H. Morkoc, H. Unlu, and G. Ji, *Principles and Technology of MODFETS* (Wiley, New York, 1991), p. 358.
[23]S. M. Sze, *Physics of Semiconductor Devices* (Wiley, New York, 1981), p. 343.
[24]B. D. Hoffman and R. A. Adomaitis, IEEE J. Semicond. Manuf. (submitted, 2004).
[25]*Bede Control v.2.1 User's Manual* (Bede Scientific Inc., Englewood, 1998), p. 29.
[26]*Transpector CPM Operating Manual* (Inficon, Inc., Syracuse, 2003), p. 3.23.
[27]NIST Chemistry Webbook Database, http://webbook.nist.gov/chemistry.
[28]*International Technology Roadmap for Semiconductors 2003 Edition: Metrology* (International Sematech, Austin, TX, 2003).